

## ORIGINAL ARTICLE

# Tuning the endothelial response: differential release of exocytic cargos from Weibel-Palade bodies

T. D. NIGHTINGALE,\* J. J. MCCORMACK,† W. GRIMES,†‡ C. ROBINSON,\* M. LOPES DA SILVA,† I. J. WHITE,† A. VAUGHAN,† L. P. CRAMER†§ and D. F. CUTLER\*

\*Centre for Microvascular Research, William Harvey Research Institute, Barts and the London School of Medicine and Dentistry, Queen Mary University of London; †MRC Laboratory of Molecular Cell Biology, University College London, London, UK; ‡Imaging Informatics Division, Bioinformatics Institute, Singapore; and §Department of Cell and Developmental Biology, University College, London, UK

**To cite this article:** Nightingale TD, McCormack JJ, Grimes W, Robinson C, Lopes da Silva M, White IJ, Vaughan A, Cramer LP, Cutler DF. Tuning the endothelial response: differential release of exocytic cargos from Weibel-Palade bodies. *J Thromb Haemost* 2018; **16**: 1873–86.

## Essentials

- Endothelial activation initiates multiple processes, including hemostasis and inflammation.
- The molecules that contribute to these processes are co-stored in secretory granules.
- How can the cells control release of granule content to allow differentiated responses?
- Selected agonists recruit an exocytosis-linked actin ring to boost release of a subset of cargo.

**Summary.** *Background:* Endothelial cells harbor specialized storage organelles, Weibel-Palade bodies (WPBs). Exocytosis of WPB content into the vascular lumen initiates primary hemostasis, mediated by von Willebrand factor (VWF), and inflammation, mediated by several proteins including P-selectin. During full fusion, secretion of this large hemostatic protein and smaller pro-inflammatory proteins are thought to be inextricably linked. *Objective:* To determine if secretagogue-dependent differential release of WPB cargo occurs, and whether this is mediated by the formation of an actomyosin ring during exocytosis. *Methods:* We used VWF string analysis, leukocyte rolling assays, ELISA, spinning disk confocal microscopy, high-throughput confocal microscopy and inhibitor and siRNA treatments to demonstrate the existence of cellular machinery that allows differential release of WPB cargo

proteins. *Results:* Inhibition of the actomyosin ring differentially effects two processes regulated by WPB exocytosis; it perturbs VWF string formation but has no effect on leukocyte rolling. The efficiency of ring recruitment correlates with VWF release; the ratio of release of VWF to small cargoes decreases when ring recruitment is inhibited. The recruitment of the actin ring is time dependent (fusion events occurring directly after stimulation are less likely to initiate hemostasis than later events) and is activated by protein kinase C (PKC) isoforms. *Conclusions:* Secretagogues differentially recruit the actomyosin ring, thus demonstrating one mechanism by which the prothrombotic effect of endothelial activation can be modulated. This potentially limits thrombosis whilst permitting a normal inflammatory response. These results have implications for the assessment of WPB fusion, cargo-content release and the treatment of patients with von Willebrand disease.

**Keywords:** exocytosis; hemostasis; inflammation; von Willebrand factor; Weibel-Palade bodies.

Correspondence: Daniel F. Cutler, MRC Laboratory for Molecular Cell Biology, Cell Biology Unit and Department of Cell and Developmental Biology, University College London, Gower Street, London WC1E6BT, UK  
Tel.: +44 20 7679 7808  
E-mail: d.cutler@ucl.ac.uk

Received: 10 April 2018

Manuscript handled by: X. Long Zheng

Final decision: P. H. Reitsma, 1 June 2018

## Introduction

A rapid response to vascular injury or infection minimizes blood loss and spread of pathogens. Endothelial rod-shaped storage organelles called Weibel-Palade bodies (WPBs) harbor multiple pre-made, pro-inflammatory and pro-hemostatic proteins [1–3], including the leukocyte receptor P-selectin, the pro-hemostatic glycoprotein von Willebrand factor (VWF), pro-inflammatory cytokines, and agents that control tonicity [4]. Some cargos are up-regulated after endothelial activation, including IL-8 [5,6] and angiopoietin-2 [7]. Within minutes of secretagogue stimulation, WPBs undergo exocytosis [8,9], releasing their content into the blood, which initiates hemostasis and leukocyte recruitment [2].

Release of VWF and P-selectin have distinct functional consequences. VWF multimers are stored in multi-concater coiled proteinaceous tubules, together with their cleaved pro-peptides [10]. Upon exocytosis, the tubules unfurl into long protein strings, which recruit platelets even at non-pathological shear [11,12]. VWF mutations or defective cellular machinery cause incorrect processing and can underlie bleeding disorders [13]. Animal models of or patients with, low VWF exhibit a decreased incidence of atherosclerosis [14]. Conversely, excess ultra-high-molecular-weight VWF in the bloodstream (due to induced or genetic absence of the VWF-cleaving metalloprotease ADAMTS-13) results in the microvascular occlusions [15] of thrombotic thrombocytopenic purpura, and patients with elevated plasma VWF have an increased risk of cardiac events [14,16] and stroke [17]. VWF is thus a key factor in cardiovascular disease. P-selectin is a leukocyte receptor that mediates initial rolling of leukocytes on the vascular endothelium [18–20]. Loss or inappropriate clustering of P-selectin at the endothelial cell surface results in immunodeficiency due to a failure to recruit leukocytes [20,21].

Being co-stored, parallel release at exocytosis of VWF and smaller components such as P-selectin should be obligatory. However, there is evidence of differential release of VWF [22–24]. At low extracellular pH, unfolding of VWF is prevented, such that only small soluble components are released [22], whereas in lingering kiss fusion, comprising about 10% of fusion events after strong histamine stimulation [23], only cargo proteins  $\leq 40$  kDa are released. However, neither of these mechanisms enables differential release of VWF vs. P-selectin and therefore the segregation of inflammatory and hemostatic effects. Furthermore, no molecular machinery providing physiological control of VWF release has been identified.

Recent research has uncovered machinery controlling the efficiency of VWF release from WPBs [9,25,26]. If differentially recruited by agonists, this would potentially promote regulated release of pro-hemostatic VWF whilst not altering release of smaller pro-inflammatory components. Such 'differential release', a novel layer of regulation, could limit potentially dangerous thrombosis whilst allowing a normal inflammatory response. We have used multiple *in vitro* assays to show that recruitment of an actomyosin ring allows differential release of cargo following stimulation by numerous physiologically relevant secretagogues. We also describe protein kinase-C as upstream machinery that modulates its recruitment.

## Methods

### *Cell culture and nucleofection*

Human umbilical vein endothelial cells (HUVECs) were cultured as described previously [27]. GFP-VWF [28] was from J. Voorberg and J.A. Van Mourik (Sanquin Research Laboratory, Amsterdam, the Netherlands).

P-sel.Lum-mCherry has been previously described [9]. Lifeact-GFP [29] was from B. Baum (University College London, London, UK). GFP-tagged PKC $\alpha$  and PKC $\beta$  were gifts from A. Poole (University of Bristol, Bristol, UK). GFP-tagged PKC $\delta$  and PKC $\epsilon$  were from P. Parker (Francis Crick Institute, London, UK). DNA (1–5  $\mu$ g) was nucleofected using program U-001 (Lonza, Slough, UK). Cells were typically assayed 24 h post-transfection.

### *Immunofluorescence*

This has been detailed previously [9].

### *Secretion assay and ELISA*

HUVECs were incubated with 1  $\mu$ mol L $^{-1}$  cytochalasin E (CCE) and 25  $\mu$ mol L $^{-1}$  blebbistatin (Sigma-Aldrich, St Louis, MO, USA) for 5–15 min before determining VWF or pro-peptide release in the presence or absence of 100 ng mL $^{-1}$  phorbol 12-myristate 13-acetate (PMA) (Sigma-Aldrich), 100  $\mu$ mol L $^{-1}$  histamine or 100  $\mu$ mol L $^{-1}$  histamine/10  $\mu$ mol L $^{-1}$  adrenalin/100  $\mu$ mol L $^{-1}$  3-isobutyl-1-methyl xanthine (IBMX) and/or the relevant drug for 30 min. VWF secretion assay and ELISAs have been described previously [30,31]. For VWF pro-peptide secretion an ELISA kit (Mast Group Ltd, Bootle, Merseyside, UK) was used according to the manufacturer's instructions.

### *Exocytic site labelling assay*

Exocytic site labelling was performed using a modified method from Knop and Gerke [32]. Confluent cells grown on 96-well plates (Nunc, Roskilde, Denmark) for 2 days were washed in prewarmed release medium (M199 with 0.2% bovine serum albumin [BSA] and 10 mmol L $^{-1}$  HEPES), and where necessary incubated with CCE or blebbistatin as for secretion assays. Cells were incubated for 2–20 min in the presence of rabbit anti-VWF and either unstimulated or stimulated with phorbol 12-myristate 13-acetate (PMA) (6.25–100 ng mL $^{-1}$ ), histamine (100  $\mu$ mol L $^{-1}$ ), thrombin (1 U  $\mu$ L $^{-1}$ ), vascular endothelial growth factor (VEGF) (40 ng mL $^{-1}$ ), Forskolin (10  $\mu$ mol L $^{-1}$ ), ATP (100  $\mu$ mol L $^{-1}$ ) or adrenalin (10  $\mu$ mol L $^{-1}$ )/IBMX (100  $\mu$ mol L $^{-1}$ ), either alone or in combination, in release medium. Cells were incubated with wheat germ agglutinin (Thermo Fisher Scientific, Waltham, MA, USA) for 2 min on ice or fixed immediately in 4% paraformaldehyde, permeabilised with 0.2% Triton X-100 in PBS and incubated with mouse anti-VE-cadherin (BD Biosciences, Franklin Lakes, NJ, USA) or with secondary antibodies conjugated to Alexa Fluor 488-nm or 647-nm and Hoescht 33342.

### *High-throughput image acquisition and segmentation*

Cells were cultured, fixed and stained in 96-well plates, then imaged with the Opera high-content screening

(PerkinElmer, Waltham, MA, USA) confocal microscope using a 40× air objective lens (NA 0.6). Datasets comprise 864 images (nine fields of view per well), approximately 10 000 cells. Analysis used Python2.7 with the scikit-image library [33]. Image noise was reduced by Gaussian blurring, then a binary mask was created using a threshold value from moment-preserving thresholding [34]. Adjacent sites were split using the marker-based watershed flooding algorithm. Segmented objects beneath the resolution limit of the optical system were removed. Finally, morphometric measurements were taken. Segmentation was validated by comparison with a set of manually annotated images. Data analysis was conducted in the R programming language version 3.2 [35].

#### *Western blotting*

This was carried out as described previously [9].

#### *Live-cell imaging*

Nucleofected cells stimulated with PMA, histamine or histamine/adrenalin/IBMX were visualized as detailed previously using a 100× oil immersion lens (NA 1.4) on a spinning-disk system (UltraVIEW VoX; PerkinElmer) [9].

#### *VWF string analysis and quantification*

String assays were carried out as described previously [9].

#### *Rolling assay and quantification*

HUVECs prepared as for string assays were placed on the stage of an Axiovert 200M microscope at 37°C, connected to a syringe pump, and Hanks Balanced Salts Solution (HBSS) perfused for 2 min at a constant wall shear stress 0.07 Pa (0.7 dyne cm<sup>-3</sup>). HUVECs were then either perfused with HBSS alone or stimulated with histamine/adrenalin/IBMX in the presence or absence of CCE (0.25 μmol L<sup>-1</sup>) for 5 min before being perfused with THP-1 cells (0.5 × 10<sup>6</sup>/ml) in HBSS in the presence or absence of secretagogue. Videos were recorded using a Rolera Bolt CMOS camera (Ziosoft, Tokyo, Japan) using MicroManager software. Videos were analysed using ImageJ. Interacting THP-1 cells were defined as those seen to pause on the endothelial monolayer and counted manually.

#### *Cell surface biotinylation assay*

This was carried out as described previously [21].

## **Results**

We and others demonstrated that VWF release is boosted by a contractile actomyosin ring forming around the fused WPB to squeeze out content [9,25,26], but whether

this boost affects platelet and leukocyte recruitment to endothelial cells was undetermined. We first analyzed the effect of actomyosin ring inhibition on VWF string formation (Fig. 1A–C). HUVECs grown in flow chambers were briefly treated with a low dose (thus without an effect on cell viability or adherence) of the actin depolymerising drug CCE, which binds to the barbed end of the actin chain [36]. A cocktail (to stimulate both calcium and cAMP-mediated pathways of WPB exocytosis) of histamine, adrenalin and 3-isobutyl-1-methyl xanthine (IBMX) was used to stimulate WPB exocytosis and the length of resulting strings was analyzed. In cells treated with CCE the formation of long strings was significantly reduced (Fig. 1A–C). To determine if leukocyte recruitment is also reduced we monitored rolling in the presence or absence of CCE. We saw no significant difference in the frequency of rolling leukocytes following drug treatment (Fig. 1D; Videos S1–S3). Thus in a controlled system, inhibition of the actomyosin ring differentially affects inflammatory vs. hemostatic functioning. We hypothesize that the regulation of VWF secretion by the actomyosin ring is a secretagogue-dependent way to bias the endothelial response to be more or less hemostatic.

Von Willebrand factor is by far the largest WPB cargo protein and is likely to require the most physical force for efficient release, potentially explaining why control of the actin ring specifically affects hemostatic responses. Similarly, smaller pro-inflammatory content should be less affected by actin ring inhibition (Fig. 2A,B). Further, to provide physiological regulation, different secretagogues should differentially utilize the actin ring. To test this we used three secretagogues that activate different downstream signaling pathways [4]: PMA, histamine and histamine/adrenalin/IBMX. To determine the effect of content size on its efficiency of release, we compared secretion of VWF (large cargo) (Fig. 2Ci) with VWF pro-peptide (small cargo) (Fig. 2Cii). The pro-peptide is necessarily co-packaged in equimolar amounts with VWF, thus providing exact ratiometric data. Further, the pro-peptide is increasingly used clinically to determine VWF clearance [37], thus evidence of its differential release is of intrinsic interest. Although PMA and histamine/adrenalin/IBMX were similarly effective at exocytosing both large and small content, histamine releases the large cargo VWF much less efficiently than PMA. This was most clearly apparent when presented as the ratio of VWF/pro-peptide release to give a measure of the secretion efficiency of large vs. small cargo (Fig. 2Ciii).

To determine if this difference in efficiency depends on the actomyosin machinery we used CCE to inhibit actin polymerization and blebbistatin [38] to block non-muscle myosin II contraction (Fig. 2D). CCE completely inhibits ring formation, whereas blebbistatin reduces the rate of ring contraction. As predicted, efficient release of VWF following PMA stimulation requires the actomyosin ring; these inhibitors reduced VWF release (Fig. 2Di).

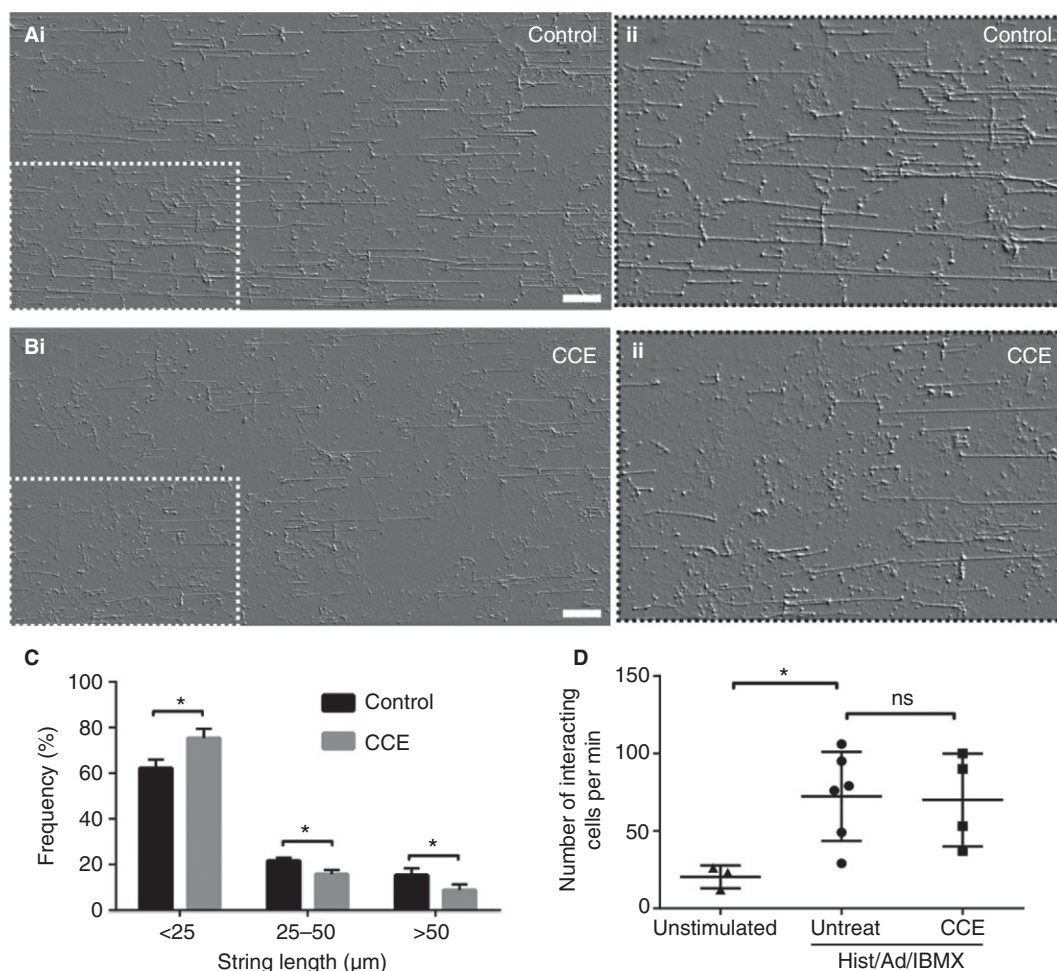


**Fig. 1.** The actomyosin ring increases the efficiency of von Willebrand factor (VWF) string formation but has little effect on leukocyte rolling. Human umbilical vein endothelial cells (HUVECs) stimulated under flow with histamine ( $100 \mu\text{mol L}^{-1}$ )/adrenalin ( $10 \mu\text{mol L}^{-1}$ )/IBMX ( $100 \mu\text{mol L}^{-1}$ ) in the presence or absence of  $0.25 \mu\text{mol L}^{-1}$  cytochalasin E (CCE) and fixed for string length analysis (A–C) or perfused with THP-1 leukocytes for rolling analysis (D) ( $n = 3$ ). (A, B) HUVECs were fixed and stained for VWF before imaging on a confocal microscope; pictures shown are tile scans of 10 fields of view. The whole image (i) and with the boxed area magnified (ii) are shown with a filter added to improve contrast. Scale bar  $50 \mu\text{m}$ . (C) The lengths of VWF strings were quantified from three independent experiments (control,  $n = 13$  images, 1346 strings; CCE,  $n = 14$  images, 1364 strings). The percentage of strings less than  $25 \mu\text{m}$ , between  $25$  and  $50 \mu\text{m}$  and longer than  $50 \mu\text{m}$  was calculated per image and standard error of the mean (SEM) shown. (D) The number of interacting THP-1 leukocytes/min was determined from movies. Each point represents the total number of interacting leukocytes per 1-min movie, with up to two movies acquired per experiment from stimulated cells. Error bars represent standard deviation (SD). Statistical significance assessed using the Mann–Whitney test (C) and one-way ANOVA with Dunnett’s multiple comparison test (D).  $*P \leq 0.05$ .

Conversely, release of the smaller VWF pro-peptide is essentially actin ring independent (Fig. 2Dii). The ratio of VWF to pro-peptide release following PMA stimulation is  $0.4 \pm 0.05$ , whereas in cells that cannot recruit the ring, efficiency of release falls to  $0.2 \pm 0.04$  (Fig. 2Diii). Interestingly, PMA-stimulated cells in which the actin ring is inhibited behave similarly to histamine-stimulated cells in terms of efficiency of VWF release. These data show that the actomyosin ring provides a means for secretagogue-dependent control of VWF release without affecting smaller cargo.

We next addressed whether the actomyosin ring influenced the delivery of integral membrane proteins to the cell surface from WPBs. We stimulated HUVECs with

different secretagogues and monitored P-selectin appearance on the plasma membrane (Fig. 3A,C). The most efficient delivery to the plasma membrane occurred following PMA stimulation, whereas histamine and histamine/adrenalin/IBMX behave similarly. The delivery of P-selectin to the cell surface in response to PMA was partially dependent on the actomyosin ring as both blebbistatin and CCE reduced cell surface levels (Fig. 3B,D). The reason for this is unclear but might reflect VWF/P-selectin binding, retaining P-selectin within the WPB after fusion [39]. Consistent with this, as reported, P-selectin is enriched along VWF strings [40] and at exocytic sites post-exocytosis (Figure S1 and Fig. 3E). Alternatively, the partial inhibition could

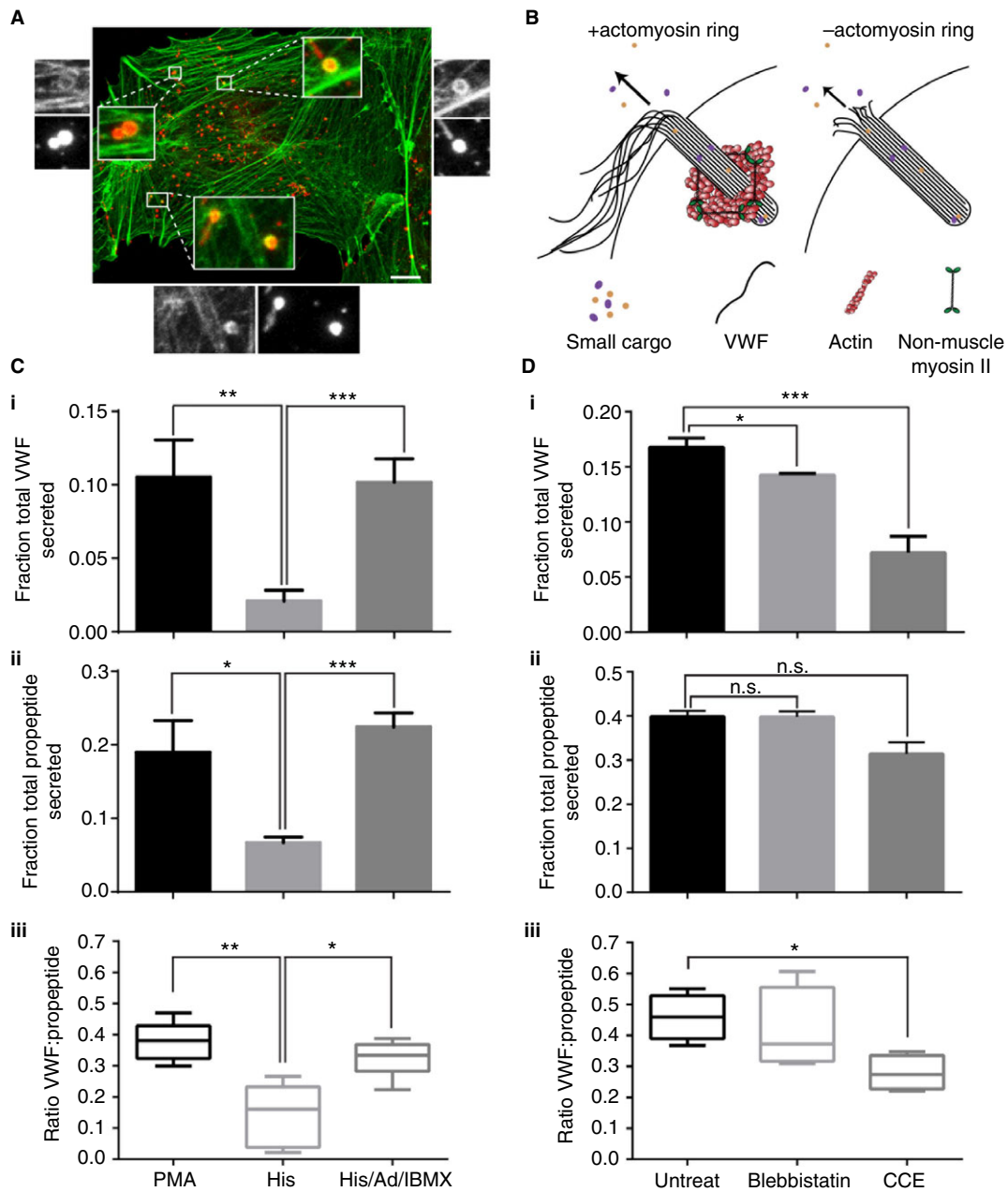


**Fig. 2.** Different secretagogues release von Willebrand factor (VWF) and VWF pro-peptide with differing efficiencies in a manner that is dependent on the actomyosin ring. (A) Human umbilical vein endothelial cells (HUVECs) were stimulated with  $100 \text{ ng mL}^{-1}$  phorbol 12-myristate 13-acetate (PMA) for 5 min and fixed using a procedure optimal for the actin cytoskeleton, co-stained for VWF (red) and phalloidin (green) and imaged on a confocal microscope. Maximum intensity projections shown. Boxed regions are shown magnified. Bar  $10 \mu\text{m}$ . (B) Schematic of Weibel-Palade body exocytosis in the presence or absence of an actomyosin ring. Small cargo release is ring independent, whereas VWF release is more efficient in the presence of the ring. (C) Quantification of PMA ( $100 \text{ ng mL}^{-1}$ ), histamine ( $100 \mu\text{mol L}^{-1}$ ) or histamine ( $100 \mu\text{mol L}^{-1}$ )/adrenalin ( $10 \mu\text{mol L}^{-1}$ )/3-isobutyl-1-methyl xanthine ( $100 \mu\text{mol L}^{-1}$ )-stimulated (Ci) VWF or (Cii) pro-peptide secretion ( $n = 6-9$ ); error bars = SEM. (Ciii) Ratio of stimulated VWF:propeptide release. Boxes represent 25th–75th percentiles; whiskers represent minimum and maximum values. (D) Quantification of PMA ( $100 \text{ ng mL}^{-1}$ )-stimulated (Di) VWF or (Dii) pro-peptide secretion in the presence or absence of  $25 \mu\text{mol L}^{-1}$  blebbistatin or  $1 \mu\text{mol L}^{-1}$  cytochalasin E ( $n = 4$ ); error bars = standard error of the mean (SEM). (Diii) Ratio of stimulated VWF:propeptide release. Error bars = SEM. Statistical significance assessed using *t*-test with Welch's correction (Ci-ii and Di-ii) and ratio *t*-test (Ciii and Diii). \* $P \leq 0.05$ , \*\* $P \leq 0.01$  and \*\*\* $P \leq 0.001$ . [Color figure can be viewed at [wileyonlinelibrary.com](http://wileyonlinelibrary.com)]

reflect a steric hindrance of the extracellular domain of P-selectin as it exits the fusion pore; P-selectin mobility is limited in mature WPBs [41]. Therefore, the delivery

of larger integral membrane proteins can be influenced by inhibition of the actin ring, although not enough to inhibit function (Fig. 1D).

To directly determine the extent and kinetics of actin ring recruitment, we monitored actin ring recruitment in live cells [9]. We monitored the loss of mcherry-Pselectin-lum (marking WPB fusion) and the recruitment of lifeact-GFP (tracking ring assembly) and found (Fig. 4A) that approximately  $\approx 15\%$  of histamine-stimulated fusion events,  $\approx 40\%$  of histamine/adrenalin/IBMX-stimulated events and  $\approx 65\%$  of PMA-stimulated events recruit the ring. Additionally, the probability of ring recruitment increases over time (Fig. 4B). Immediately following stimulation (0–50 s), and irrespective of secretagogue, the likelihood of recruitment is low. For PMA and histamine/adrenalin/IBMX-stimulated cells this is followed by increased ring recruitment (50–200 s) (68% and 69% of

events are actin-positive in PMA and histamine/adrenalin/IBMX-stimulated cells, respectively, over 100–600 s). In histamine-stimulated cells the majority of events are actomyosin ring independent, although the percentage of actin-positive events increases over time, until every event recruited a ring (although few events occur at these later times). Therefore time-dependent phenomena are likely to be required for ring recruitment, presumably including both signaling and recruitment of machinery.

We next sought to determine whether recruitment of the actomyosin ring following stimulation by the many established WPB secretagogues [4,42], both alone and in combination, is a major feature of exocytosis. We developed an assay for determination of the size of the fusion

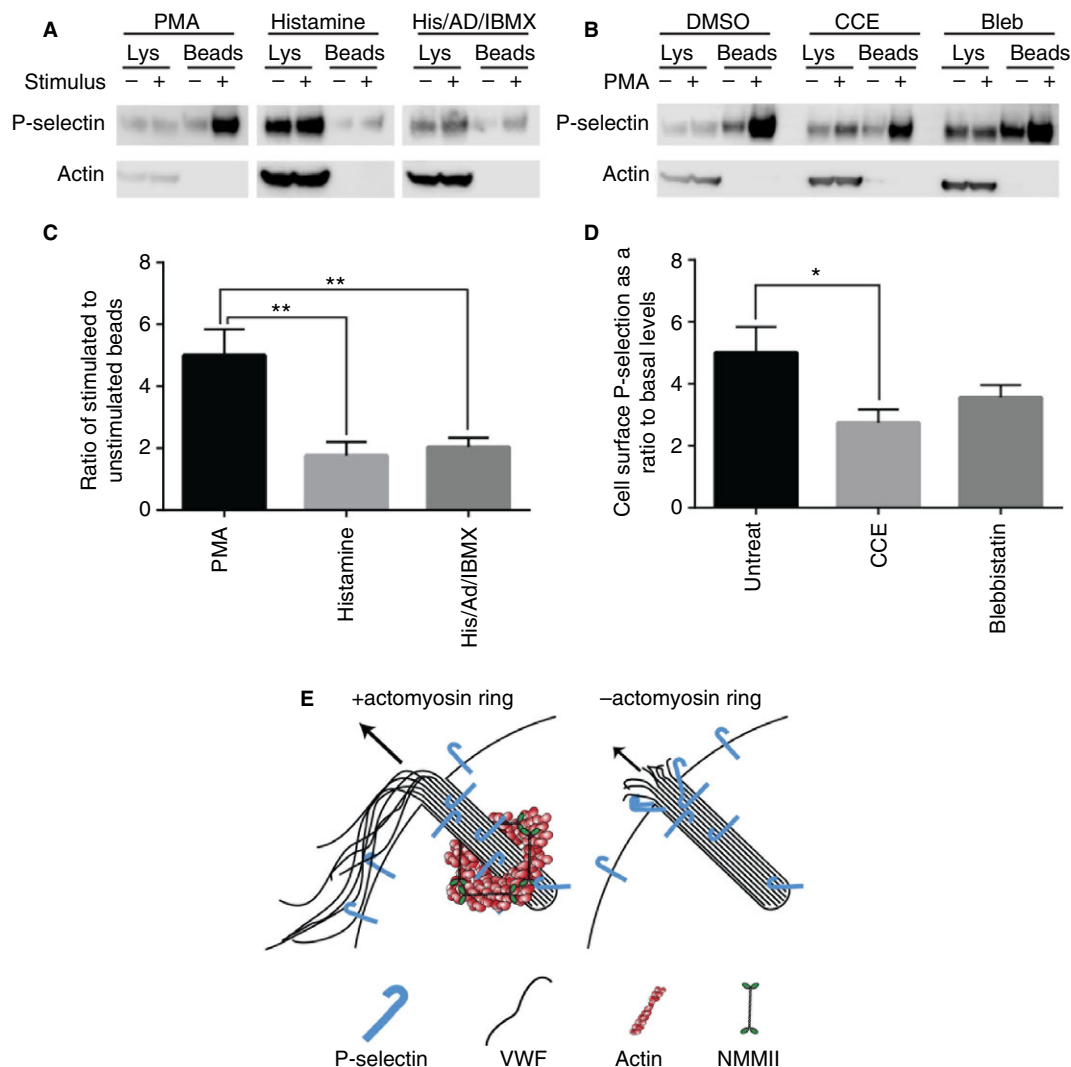


**Fig. 3.** Release of P-selectin from WPBs for recruitment to the plasma membrane is partially ring dependent. The proportion of cell surface to total P-selectin levels was determined by surface biotinylation and neutravidin pulldown following stimulation with PMA (100 ng mL<sup>-1</sup>) (A, B), histamine (100  $\mu$ mol L<sup>-1</sup>) or histamine (100  $\mu$ mol L<sup>-1</sup>)/adrenalin (10  $\mu$ mol L<sup>-1</sup>)/IBMX (100  $\mu$ mol L<sup>-1</sup>) (A) or following PMA stimulation in the presence or absence of 25  $\mu$ mol L<sup>-1</sup> blebbistatin or 1  $\mu$ mol L<sup>-1</sup> CCE (B). Quantification of Western blots shown (C) PMA  $n = 11$ , his  $n = 3$ , HAI  $n = 6$ , (D)  $n = 12$ . (C, D) Error bars = standard error of the mean (SEM). Statistical significance assessed using *t*-test with Welch's correction (C, D). \* $P \leq 0.05$ , \*\* $P \leq 0.01$ . (E) Schematic of WPB exocytosis in the presence or absence of an actomyosin ring. WPB, Weibel-Palade body; NMMII, non-muscle myosin II. [Color figure can be viewed at [wileyonlinelibrary.com](http://wileyonlinelibrary.com)]

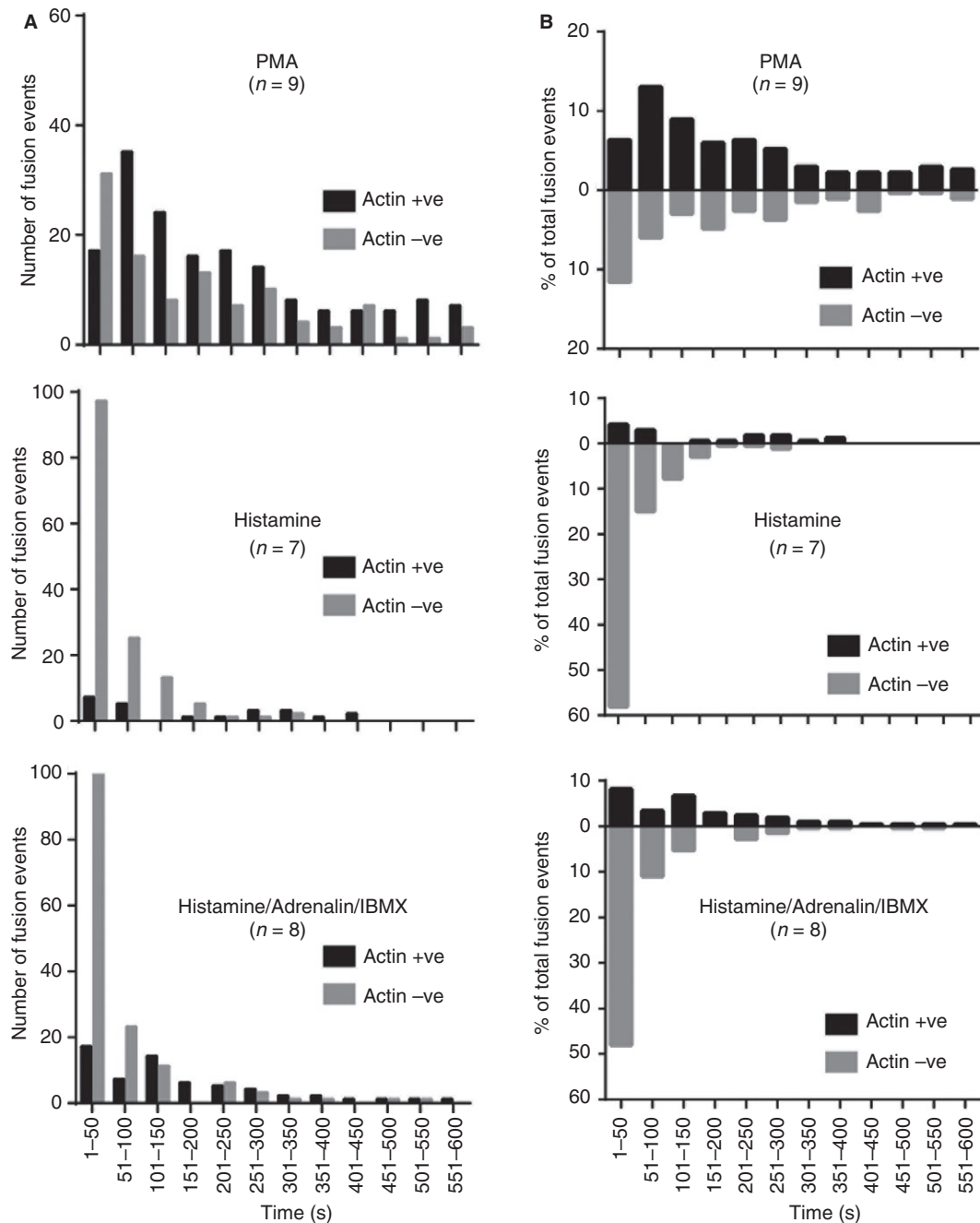


**Fig. 4.** Actin ring recruitment is secretagogue and time dependent. Human umbilical vein endothelial cells (HUVECs) were nucleofected with mCherry-PselectinLum domain and lifeactGFP and imaged with a spinning-disk confocal microscope in the presence of  $100 \text{ ng mL}^{-1}$  PMA ( $n = 9$ ),  $100 \mu\text{mol L}^{-1}$  histamine ( $n = 7$ ) or  $100 \mu\text{mol L}^{-1}$  histamine/ $10 \mu\text{mol L}^{-1}$  adrenalin/ $100 \mu\text{mol L}^{-1}$  IBMX ( $n = 8$ ). Z stacks were acquired at a spacing of  $0.5 \mu\text{m}$  every 5 s for 10 min. (A) The frequency of fusion events with (positive +ve) or without an actin ring (negative -ve) at each time-point is plotted. (B) The percentage of actin ring-positive (+ve) or negative events (-ve) compared with the total number of events is plotted.

site. This assay takes advantage of information obtained previously using correlative light and electron microscopy and scanning electron microscopy showing that levels of exocytosed, antibody-accessible VWF are dependent on the actomyosin ring [9]. We added anti-VWF antibody to the media to retain VWF at exocytic sites (and prevent string formation) [32,43] to analyze

exocytic site formation in thousands of cells. We hypothesized that more efficient release mediated by the actin ring is likely to result in bigger sites (Fig. 5B), and developed an automated segmentation protocol to acquire a set of morphological measurements for each site from 72 fields of view (950–1200 cells) analyzed per condition (Fig. 5A).

This approach is unbiased, automated and highly sensitive, as shown by our analyses revealing that the number of sites increased in response to increased PMA in a dose-dependent manner (Figure S2Aa), without change to the site area (Figure S2Ab). Thus, even at a high density, segmentation of individual sites is not compromised. Histamine elicits a rapid response, typically complete by 10 min post-stimulation, whereas PMA produces a more linear release of VWF [44]. Importantly, these biochemical dynamics were replicated in our assay, which is

sensitive enough to distinguish differences in the number of exocytic sites over discrete 2-min periods (Fig. 5C). To verify the assay could differentiate ring-dependent and independent exocytic events, we monitored the number (Fig. 5D) and area of sites (Fig. 5E) and noted that sites segmented from stimulated cells were significantly larger than those from unstimulated cells, and that PMA-stimulated cells produce larger sites than histamine-stimulated cells, correlating with actin ring recruitment. We therefore analyzed changes in histamine and PMA-stimulated cells

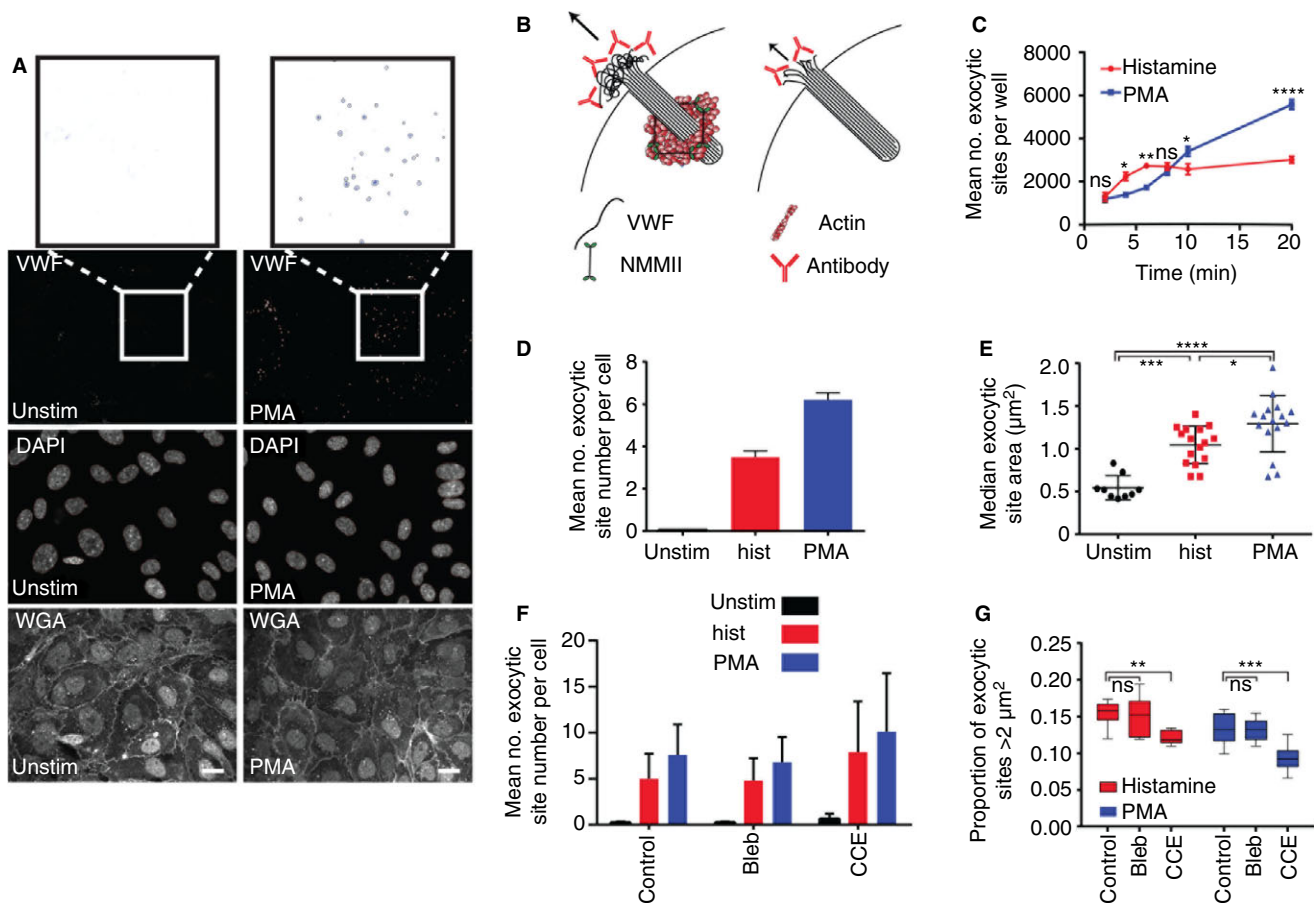


**Fig. 5.** High-throughput analysis of exocytic events. (A) Human umbilical vein endothelial cells (HUVECs) were unstimulated or stimulated with  $100 \text{ ng } \mu\text{L}^{-1}$  PMA for 10 min, followed by staining for external von Willebrand factor (VWF), plasma membrane with wheat germ agglutinin (WGA) and the nucleus (DAPI, 4',6-diamidino-2-phenylindole). Nine fields of view were acquired per well and eight wells imaged per condition. External VWF was segmented using a custom-designed program. Boxed areas on the VWF channel are shown inverted and at higher magnification as examples of segmented sites typically acquired from unstimulated and PMA-stimulated cells. Scale bar  $20 \mu\text{m}$ . (B) Schematic of external antibody labelling protocol to differentiate between actomyosin-dependent and independent exocytosis. NMMII, non-muscle myosin II. (C) HUVECs stimulated with either histamine ( $100 \mu\text{mol L}^{-1}$ ) or PMA ( $100 \text{ ng mL}^{-1}$ ) were fixed following 2–20 min of stimulation. The number of segmented external exocytic sites was calculated for each well (the sum of nine fields of view) for each time-point and mean and standard error plotted ( $n = 8$  wells). A representative experiment is shown from  $n = 4$  independent experiments. (D and E) HUVECs were stimulated for 10 min with PMA ( $100 \text{ ng mL}^{-1}$ ) or histamine ( $100 \mu\text{mol L}^{-1}$ ) or left unstimulated. The mean number of exocytic sites per cell per well (D) ( $n = 8$  wells, a representative experiment is shown from  $n = 3$  independent experiments) and the median area per site (E) ( $n = 9$ –16 independent experiments) are shown. Bars represent standard error of the mean (SEM). (F and G) HUVECs were untreated or pretreated with blebbistatin ( $25 \mu\text{mol L}^{-1}$ ) or cytochalasin E (CCE) ( $1 \mu\text{mol L}^{-1}$ ) for 15 min before stimulation with histamine and PMA. The mean number of sites per cell (F) ( $n = 3$  independent experiments) and the proportion of sites with area greater than  $2 \mu\text{m}^2$  (G) ( $n = 8$  wells, a representative experiment from  $n = 3$  independent experiments is shown). Boxes represent 25th–75th percentiles; whiskers represent minimum and maximum values. Statistical significance was assessed using two-way ANOVA with Sidak's multiple comparison test (C and G), or one-way ANOVA with Tukey's multiple comparison test (E). \* $P \leq 0.05$ , \*\* $P \leq 0.01$ , \*\*\* $P \leq 0.001$ , \*\*\*\* $P \leq 0.0001$ . [Color figure can be viewed at [wileyonlinelibrary.com](http://wileyonlinelibrary.com)]

treated with blebbistatin and CCE to determine the effect of actin ring inhibition on the proportion of large exocytic sites (classified as those greater than  $2 \mu\text{m}^2$ ) (Fig. 5G and Figure S2B). CCE treatment specifically reduces the proportion of larger exocytic sites following both PMA and histamine stimulation, whereas blebbistatin, as expected, had little effect (as it slows rather than completely inhibits actomyosin ring contraction). This effect was greatest in PMA-stimulated cells (Fig. 5G and Figure S2B). Together these results validate a new, sensitive, high-throughput method of monitoring VWF exocytic sites suitable for screening secretagogues for their ability to recruit the actomyosin ring.

We then surveyed different secretagogues for their use of the actomyosin ring. By determining the number (Fig. 6A and Figure S3A,B) and size of exocytic sites (Fig. 6B–D and Figure S3C,D) following stimulation with different secretagogues in isolation or combination, we found significant differences in actin ring recruitment (Fig. 6C,D, and Figure S3C–F). Although thrombin relies minimally on the actin ring for release of VWF, PMA, VEGF, histamine/adrenalin/IBMX and forskolin are strong ring recruiters (correlating with our and others' findings [9,25]). We also find that actin ring recruitment can be enhanced via addition of some, but not all, calcium or cAMP-raising agents (Fig. 6 and Figure S3), which is consistent with our earlier ELISA data. Our approach provides large quantitative datasets to reveal actin ring-dependence for a range of secretagogues and indicates for the first time that endothelial cells, by responding to physiological cues, have the capability to tune the release of cargo content.

We next sought the upstream machinery required for actin ring recruitment. Actin-dependent exocytic structures occur in the cortical granules of *Xenopus* oocytes, the zymogen granules of the pancreatic and parotid acinar and the lamellar bodies of type II pneumocytes [45]. Some of these granules utilize protein kinase C (PKC) isoforms to recruit an actin ring [46,47]. Given this, and that PMA (an activator of classical and non-classical PKC isoforms) recruits the actin ring most efficiently, we analyzed the role of PKC in ring recruitment.

PKC $\alpha$ , PKC $\delta$ , PKC $\epsilon$ , PKC $\eta$  and PKC $\zeta$  are expressed in HUVECs [48]. Live-cell imaging of individual fusion events using mCherry-P-selectinLum as a marker of fusion and various human GFP-tagged versions of PKC showed recruitment of PKC $\alpha$  and PKC $\delta$  on the actin ring (Fig. 7A,B) but not epsilon or beta (not endogenously expressed; data not shown), suggesting specific recruitment. Recruitment of PKC prior to the actin ring is consistent with a role upstream of or during initiation of ring recruitment (Figure S4). To assess the function of these isoforms in VWF release from PMA-stimulated cells we depleted either PKC $\alpha$  or PKC $\delta$  (Fig. 7C) and monitored VWF release by ELISA. PKC $\alpha$  but not PKC $\delta$  knock-down had a marked effect (Fig. 7D).

Finally, we monitored the effect of an inhibitor of PKC $\alpha$  on VWF secretion (Fig. 7E). Predictably, PKC $\alpha$  inhibition had the strongest effect on PMA-stimulated release, a lesser effect on histamine/adrenalin/IBMX-stimulated release and no effect on histamine-stimulated release (Fig. 7E and Figure S5A). We also noted some reduction in the number of exocytic sites seen in PMA-stimulated cells, with a lesser effect on histamine or histamine/adrenalin/IBMX (Figure S5B,C). An additional role for PKC in exocytosis is thus possible alongside the formation of the actomyosin ring.

## Discussion

We present here evidence for the differential release of WPB cargo that we speculate can allow the separation of hemostatic and inflammatory responses. We find that different secretagogues are differentially effective at recruiting an actomyosin ring to WPBs at exocytosis, and that recruitment of this ring correlates with the release of the largest WPB cargo protein, VWF. Ultimately this represents a new layer of control to facilitate greater regulation over the outcome of endothelial activation.

We firstly demonstrated that two functions ascribed to WPB cargo content can be differentially regulated. We used an *in vitro* flow chamber to separate effects on leukocyte adhesion from VWF string formation in endothelial cells treated with a low dose of the actin poison CCE. Recruitment of the actomyosin ring affected VWF string formation (and therefore the efficiency of platelet recruitment) (Fig. 1A–C) but not leukocyte recruitment (Fig. 1D).

To determine if this effect reflects size-specific control of the release of WPB cargo, we monitored release of equimolar co-packaged VWF multimers (large protein) vs. VWF pro-peptide (small protein) in parallel. We found that only the release of VWF was differentially evoked by secretagogues, and that this correlated with the recruitment of an actin ring (Fig. 2). Stimulation with histamine alone was not efficient at releasing VWF relative to the pro-peptide, whereas PMA or histamine/adrenalin/IBMX were much more efficient (Fig. 2C). Similar reductions in efficiency followed perturbation of actomyosin ring function at PMA stimulation plus blebbistatin or CCE (Fig. 2D); squeezing by the actin ring is more important for larger cargoes than small ones, and this can explain some of the differences revealed by functional assays. The greater effects of CCE than blebbistatin probably reflect the fact that CCE inhibits ring formation whereas blebbistatin only slows the rate of its contraction.

Leukocyte rolling following secretagogue stimulation is initiated by P-selectin [19,20] clustered at the cell surface by the WPB co-cargo CD63 [21]. CD63 readily transfers to the plasma membrane even in situations where VWF

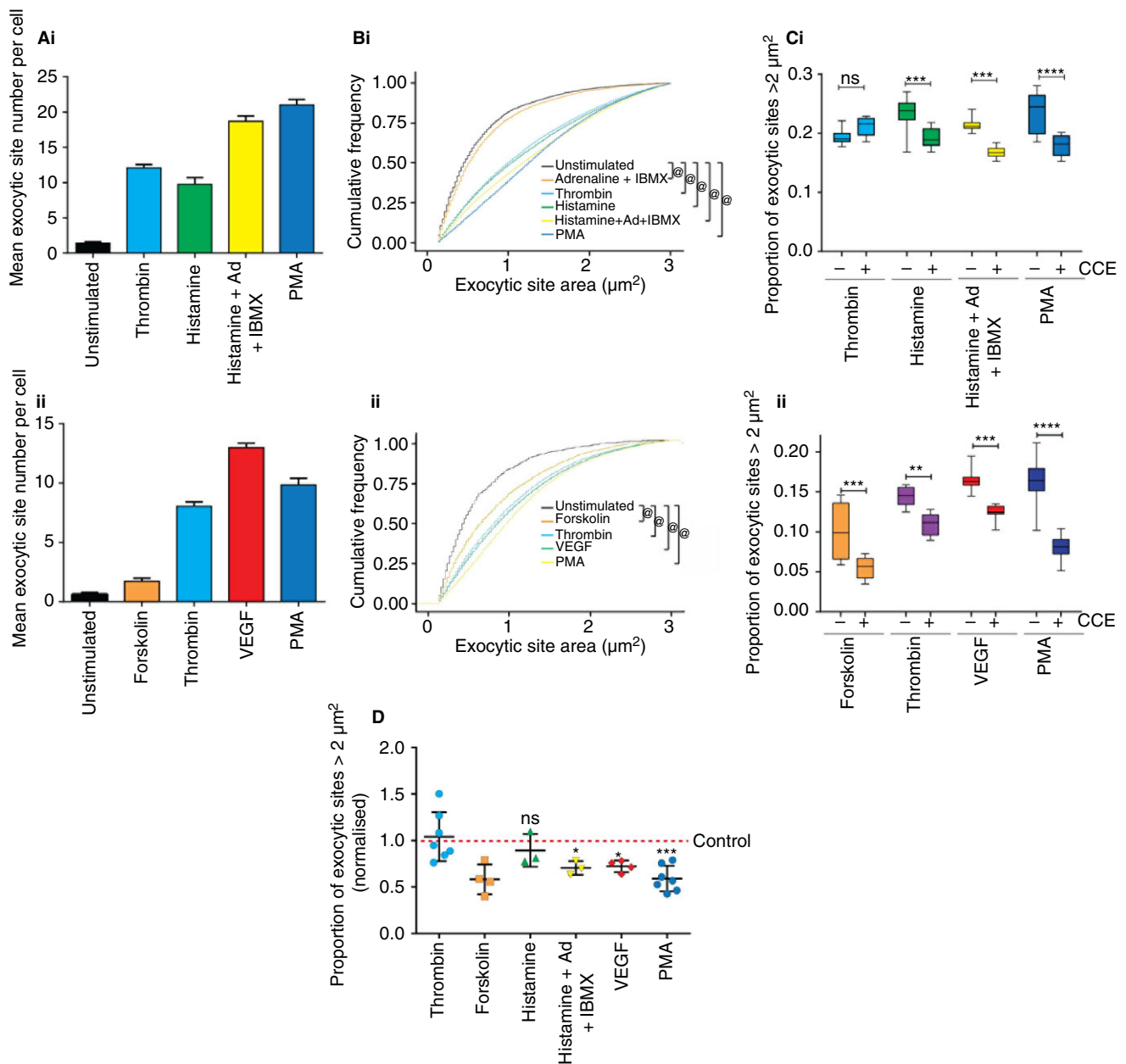


**Fig. 6.** Analysis of actin ring function with a variety of secretagogues. Human umbilical vein endothelial cells (HUVECs) were treated with or without  $1 \mu\text{mol L}^{-1}$  cytochalasin E (CCE) before being stimulated with  $100 \text{ ng } \mu\text{L}^{-1}$  PMA,  $100 \mu\text{mol L}^{-1}$  histamine,  $1 \text{ U mL}^{-1}$  thrombin,  $10 \mu\text{mol L}^{-1}$  adrenalin/ $100 \mu\text{mol L}^{-1}$  IBMX,  $100 \mu\text{mol L}^{-1}$  histamine/ $10 \mu\text{mol L}^{-1}$  adrenalin/ $100 \mu\text{mol L}^{-1}$  IBMX,  $10 \mu\text{mol forskolin}/100 \mu\text{mol L}^{-1}$  IBMX, or  $40 \text{ ng mL}^{-1}$  vascular endothelial growth factor (VEGF) for 10 min, followed by staining for external von Willebrand factor (VWF) and the nucleus. Nine fields of view were acquired per well, and eight wells imaged per condition. Data from representative experiments shown (A–C) ( $n = 3$ ) and the mean of three to seven experiments (D). (A) Mean number of exocytic sites per cell per well following secretagogue stimulation. Bars are SEM ( $n = 8$  wells). (B) Cumulative frequency graph shows the distributions of the area of exocytic sites. (C) The mean proportion of exocytic VWF-positive sites with area greater than  $2 \mu\text{m}^2$  was calculated following stimulation with various secretagogues with and without CCE ( $1 \mu\text{mol L}^{-1}$ ). Boxes represent 25th–75th percentiles; whiskers represent minimum and maximum values.  $n = 8$  wells. (D) The mean proportion of exocytic sites with area greater than  $2 \mu\text{m}^2$  following stimulation with a number of secretagogues in the presence of CCE normalized to the mean proportion of large sites in control samples. Mean value is derived from the  $n = 8$  wells per experiment ( $n = 3–7$ ). Statistical significance assessed between stimulated and unstimulated distributions using a two-sample Kolmogorov–Smirnov test (B), two-way ANOVA with Sidak’s multiple comparison test (C) and one-way ANOVA with Dunnett’s multiple comparisons test (D). \* $P \leq 0.05$ , \*\* $P \leq 0.005$ , \*\*\* $P \leq 0.001$ , \*\*\*\* $P \leq 0.0001$ , @ $P \leq 10^{-15}$ . [Color figure can be viewed at [wileyonlinelibrary.com](http://wileyonlinelibrary.com)]

release is inhibited, including release at low pH [22] or during lingering kiss fusion [23]. Surface biotinylation demonstrated that P-selectin traffic to the cell surface is

partially actomyosin ring-dependent (Fig. 3), although we see no difference in leukocyte rolling following actomyosin ring inhibition (Fig. 1D). Direct interactions with

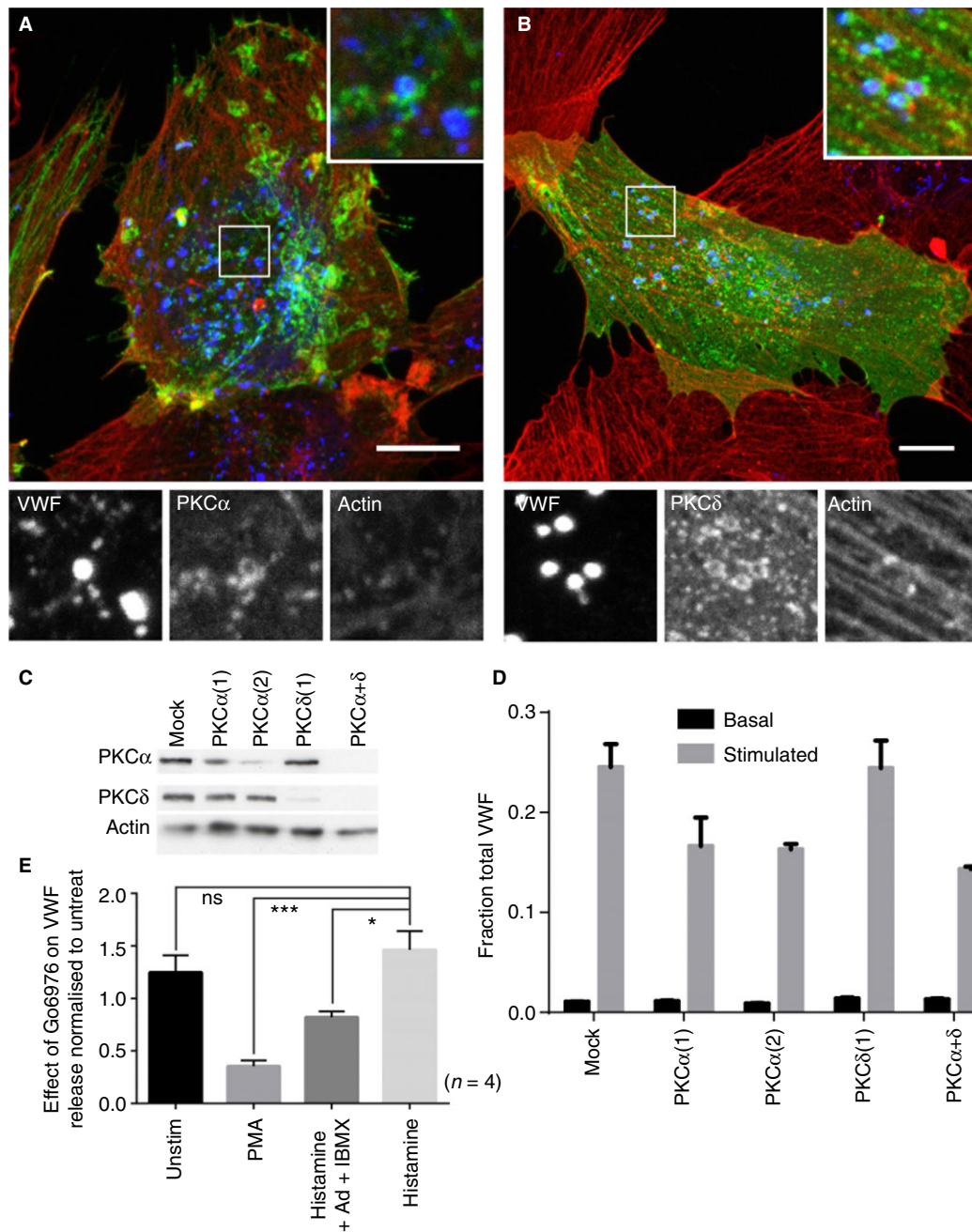


**Fig. 7.** The role of protein kinase C isoforms in actin ring recruitment and von Willebrand factor (VWF) secretion. (A, B) Human umbilical vein endothelial cells (HUVECs) were nucleofected with PKC $\alpha$ GFP (A) or PKC $\delta$ GFP (B) and stimulated for 5 min with 100 ng mL<sup>-1</sup> PMA, fixed in formaldehyde with a procedure optimal for the actin cytoskeleton, co-stained for VWF (blue) and phalloidin (red) and imaged on a confocal microscope. Image shown is a maximum intensity projection; boxed regions are shown magnified. Bar 10  $\mu$ m. (C, D) HUVECs were nucleofected with two rounds of 200 pmol siRNA against PKC $\alpha$ ,  $\delta$  or both isoforms together and either (C) the samples were prepared for Western blot or (D) VWF secretion monitored. (E) HUVECs were treated with 1  $\mu$ mol L<sup>-1</sup> GÖ6976 and then stimulated with PMA (100 ng mL<sup>-1</sup>), histamine (100  $\mu$ mol L<sup>-1</sup>) or a combination of histamine (100  $\mu$ mol L<sup>-1</sup>), adrenalin (10  $\mu$ mol L<sup>-1</sup>) and IBMX (100  $\mu$ mol L<sup>-1</sup>). VWF secretion was monitored and results are shown normalized to the uninhibited sample. The protein kinase C (PKC) inhibitor has the greatest effect on PMA-stimulated release and a lesser effect on hist/ad/IBMX.  $n = 4$ , error bars = standard error of the mean (SEM). Statistical significance assessed using  $t$ -test with Welch's correction. \* $P < 0.05$  and \*\* $P < 0.01$ . [Color figure can be viewed at [wileyonlinelibrary.com](http://wileyonlinelibrary.com)]

VWF (also suggested by imaging, Figure S1) may explain this effect [39]. The clustering effects of CD63 or a simple excess of receptor may help to mitigate the differences seen in P-selectin recruitment to the cell surface.

Directly imaging ring recruitment (Fig. 4) to determine which secretagogues recruit the ring to the greatest extent corroborated our ELISA results. Notably, we also identified a time dependence for ring recruitment, with later

exocytic events with all tested stimuli much more likely to recruit the ring. This intriguing time course suggests that downstream signaling is required both to recruit the actin ring and to localize associated cellular machinery.

The most efficient actin ring recruitment (and therefore VWF release) occurs when multiple secretagogues are used (Figs. 2 and 4). We utilized a new high-throughput approach to monitor a range of secretagogues (Figs 5, 6 and Figure S2). Assaying thousands of exocytic sites from thousands of cells, this approach affords excellent temporal sensitivity and statistical significance. *In vivo* the endothelium is likely to be stimulated by multiple secretagogues; histamine activation is accompanied by at least some adrenalin (resting levels are  $0.31 \text{ nmol L}^{-1}$  [49]). Identifying the signaling pathways downstream of secretagogue activation is complex, as many intersect. One of the strongest ring-promoting agents is the non-physiological Diacylglycerol (DAG) analogue PMA, suggesting PKC involvement (most likely PKC $\alpha$ ) (Fig. 7). Because PKC $\alpha$  can be activated directly by both DAG and calcium [50] or indirectly via cAMP-dependent agonists and EPAC (exchange proteins directly activated by cAMP isoform) [51,52], PKC activation could feasibly occur downstream of any of the ring-recruiting agonists that we, and others, have identified. The cAMP-raising secretagogues forskolin and adrenalin have previously been identified by others [25] as stimulating actin ring recruitment. Here we find that addition of adrenalin/IBMX to the calcium-dependent secretagogue histamine significantly enhances ring recruitment, suggesting that activation of cAMP may be an important route to ring recruitment. Interestingly, thrombin, which is largely actin ring independent, can inhibit cAMP production, potentially explaining why this is a poor ring recruiter [53]. However, it is likely that other, as yet unidentified, pathways independent of PKC $\alpha$  are also involved in ring recruitment. Histamine alone is able to recruit the actin ring, despite the fact that its mode of action is thought to be PKC independent [48]. Although PKC $\alpha$  acts in ring recruitment, VEGF is also effective at recruiting the actin ring and acts via PKC $\delta$  (and VWF release is not inhibited by inhibition of PKC $\alpha$  in VEGF-stimulated cells) [48], thus roles for additional PKC isoforms are possible.

Von Willebrand factor release is not completely actin ring dependent, as CCE treatment does not abolish it, and secretagogues that do not utilize the ring still expel VWF, albeit at a lower efficiency (Figs. 2–6), as measured by pro-peptide vs. VWF release. Thus, cargo expulsion may also be driven by water entry, changes in ionic fluxes or pH [54]. We have also found protracted actin ring formation and slower release of content at lowered external pH (data not shown). Other large acidified granules with viscous content including lamellar bodies, and pancreatic and parotid acinar zymogen granules all require extra machinery to drive release [45], indicating that charge is not always the sole and most efficient driving force. Other

large granules may also exhibit differential recruitment of actin rings and therefore differential release of content.

Our research complements recent research confirming that VWF release is boosted by an actomyosin ring [25,26]. However, there are differences in the findings. We concluded that rings form *de novo* after fusion [9], whereas Han *et al.* report actin remodeling before fusion from a pre-existing framework. We also differ on whether WPB localization is generally affected by myosin II inhibition [9,26]. The different conclusions might reflect which cell surface was imaged (apical vs. basal) or spinning disk vs. custom microscopy [9,25]. A role for some actin nucleation remains a possibility.

Differential release has previously been proposed, based on the presence of multiple pools of WPBs [24]. Although additional cargos can be added to WPBs, including IL-8 [5,6] and angiotensin-2 [7], we have no evidence to suggest the ring can be differentially recruited to distinct WPBs containing different cargos; this would require cytoplasmic machinery detecting cargo stored internally in WPBs.

Our results support the clinical use of VWF pro-peptide monitoring, perhaps immediately after agonist treatment, where needed. We also note that DDAVP, the secretagogue most commonly used to treat VWD patients, is cAMP-dependent [55] and perhaps this is one reason why it is an effective therapeutic choice.

In conclusion, these data provide evidence for an additional level of functional control of WPBs, concluding that endothelial cells may tune the hemostatic response via the recruitment of an actomyosin ring.

## Addendum

J. J. McCormack and T. D. Nightingale made the most substantial contributions to this paper. J. J. McCormack carried out quantification and statistical analysis of images, invented novel assays, designed and carried out experiments, analyzed data and wrote the manuscript. T. D. Nightingale invented novel assays, designed and carried out experiments, analyzed data and wrote the manuscript. C. Robinson, W. Grimes and M. Lopes da Silva designed and carried out experiments and contributed to the writing of this paper, I. J. White and A. Vaughan provided technical expertise and analyzed data, and L.P. Cramer and D.F. Cutler designed research, analyzed data and wrote the paper.

## Disclosure of Conflict of Interests

T. D. Nightingale was funded by a Medical Research Council project grant MR/M019179/1 and a British Heart Foundation project grant (PG/15/72/31732). J. J. McCormack and D. F. Cutler were funded by an MRC programme grant MC\_UU\_12018/2. I.J. White was funded by MRC LMCB core. W. Grimes was supported partly by the

Biomedical Research Council of A\*STAR (Agency for Science, Technology and Research), Singapore, partly by the MRC LMCB. C. Robinson was funded by a BHF project grant (PG/15/72/31732). M. Lopes da Silva reports grants from MRC during the conduct of the study, and grants from MRC outside the submitted work. The other authors state that they have no conflict of interest.

### Supporting Information

Additional supporting information may be found online in the Supporting Information section at the end of the article:

**Fig. S1.** P-selectin localization at exocytosis.

**Fig. S2.** High-throughput analysis of exocytic events.

**Fig. S3.** Analysis of actin ring function with a variety of secretagogues.

**Fig. S4.** The timing of PKC delta recruitment to exocytic sites.

**Fig. S5.** Effect of GÖ6976 on exit site size and number.

**Video S1.** Rolling analysis of untreated endothelial cells.

**Video S2.** Rolling analysis of endothelial cells stimulated with histamine and adrenalin.

**Video S3.** Rolling analysis of untreated endothelial cells.

### References

- 1 Metcalf DJ, Nightingale TD, Zenner HL, Lui-Roberts WW, Cutler DF. Formation and function of Weibel-Palade bodies. *J Cell Sci* 2008; **121**: 19–27.
- 2 Nightingale T, Cutler D. The secretion of von Willebrand factor from endothelial cells; an increasingly complicated story. *J Thromb Haemost* 2013; **11**(Suppl 1): 192–201.
- 3 Valentijn KM, Sadler JE, Valentijn JA, Voorberg J, Eikenboom J. Functional architecture of Weibel-Palade bodies. *Blood* 2011; **117**: 5033–43.
- 4 Rondaij MG, Bierings R, Kragt A, van Mourik JA, Voorberg J. Dynamics and plasticity of Weibel-Palade bodies in endothelial cells. *Arterioscler Thromb Vasc Biol* 2006; **26**: 1002–7.
- 5 Utgaard JO, Jahnsen FL, Bakka A, Brandtzaeg P, Haraldsen G. Rapid secretion of prestored interleukin 8 from Weibel-Palade bodies of microvascular endothelial cells. *J Exp Med* 1998; **188**: 1751–6.
- 6 Wolff B, Burns AR, Middleton J, Rot A. Endothelial cell “memory” of inflammatory stimulation: Human venular endothelial cells store interleukin 8 in Weibel-Palade bodies. *J Exp Med* 1998; **188**: 1757–62.
- 7 Fiedler U, Scharpfenecker M, Koidl S, Hegen A, Grunow V, Schmidt JM, Kriz W, Thurston G, Augustin HG. The Tie-2 ligand angiopoietin-2 is stored in and rapidly released upon stimulation from endothelial cell Weibel-Palade bodies. *Blood* 2004; **103**: 4150–6.
- 8 Erent M, Meli A, Moiso N, Babich V, Hannah MJ, Skehel P, Knipe L, Zupancic G, Ogden D, Carter T. Rate, extent and concentration dependence of histamine-evoked Weibel-Palade body exocytosis determined from individual fusion events in human endothelial cells. *J Physiol* 2007; **583**: 195–212.
- 9 Nightingale TD, White IJ, Doyle EL, Turmaine M, Harrison-Lavoie KJ, Webb KF, Cramer LP, Cutler DF. Actomyosin II contractility expels von Willebrand factor from Weibel-Palade bodies during exocytosis. *J Cell Biol* 2011; **194**: 613–29.
- 10 Springer TA. von Willebrand factor, Jedi knight of the bloodstream. *Blood* 2014; **124**: 1412–25.
- 11 De Ceunynck K, De Meyer SF, Vanhoorelbeke K. Unwinding the von Willebrand factor strings puzzle. *Blood* 2013; **121**: 270–7.
- 12 Dong JF, Moake JL, Nolasco L, Bernardo A, Arceneaux W, Shrimpton CN, Schade AJ, McIntire LV, Fujikawa K, Lopez JA. ADAMTS-13 rapidly cleaves newly secreted ultralarge von Willebrand factor multimers on the endothelial surface under flowing conditions. *Blood* 2002; **100**: 4033–9.
- 13 James PD, Lillicrap D. The molecular characterization of von Willebrand disease: good in parts. *Br J Haematol* 2013; **161**: 166–76.
- 14 van Galen KP, Tuinenburg A, Smeets EM, Schutgens RE. Von Willebrand factor deficiency and atherosclerosis. *Blood Rev* 2012; **26**: 189–96.
- 15 Zheng XL. ADAMTS13, TTP and beyond. *Hereditary Genet* 2013; **2**: e104.
- 16 Jin SY, Tohyama J, Bauer RC, Cao NN, Rader DJ, Zheng XL. Genetic ablation of Adamts13 gene dramatically accelerates the formation of early atherosclerosis in a murine model. *Arterioscler Thromb Vasc Biol* 2012; **32**: 1817–23.
- 17 Wieberdink RG, van Schie MC, Koudstaal PJ, Hofman A, Witteman JC, de Maat MP, Leebeek FW, Breteler MM. High von Willebrand factor levels increase the risk of stroke: the Rotterdam study. *Stroke* 2010; **41**: 2151–6.
- 18 Bonfanti R, Furie BC, Furie B, Wagner DD. PADGEM (GMP140) is a component of Weibel-Palade bodies of human endothelial cells. *Blood* 1989; **73**: 1109–12.
- 19 McEver RP, Beckstead JH, Moore KL, Marshall-Carlson L, Bainton DF. GMP-140, a platelet alpha-granule membrane protein, is also synthesized by vascular endothelial cells and is localized in Weibel-Palade bodies. *J Clin Invest* 1989; **84**: 92–9.
- 20 Mayadas TN, Johnson RC, Rayburn H, Hynes RO, Wagner DD. Leukocyte rolling and extravasation are severely compromised in P selectin-deficient mice. *Cell* 1993; **74**: 541–54.
- 21 Doyle EL, Ridger V, Ferraro F, Turmaine M, Saftig P, Cutler DF. CD63 is an essential cofactor to leukocyte recruitment by endothelial P-selectin. *Blood* 2011; **118**: 4265–73.
- 22 Babich V, Knipe L, Hewlett L, Meli A, Dempster J, Hannah MJ, Carter T. Differential effect of extracellular acidosis on the release and dispersal of soluble and membrane proteins secreted from the Weibel-Palade body. *J Biol Chem* 2009; **284**: 12459–68.
- 23 Babich V, Meli A, Knipe L, Dempster JE, Skehel P, Hannah MJ, Carter T. Selective release of molecules from Weibel-Palade bodies during a lingering kiss. *Blood* 2008; **111**: 5282–90.
- 24 Cleator JH, Zhu WQ, Vaughan DE, Hamm HE. Differential regulation of endothelial exocytosis of P-selectin and von Willebrand factor by protease-activated receptors and cAMP. *Blood* 2006; **107**: 2736–44.
- 25 Han X, Li P, Yang Z, Huang X, Wei G, Sun Y, Kang X, Hu X, Deng Q, Chen L, He A, Huo Y, Li D, Betzig E, Luo J. Zyxin regulates endothelial von Willebrand factor secretion by reorganizing actin filaments around exocytic granules. *Nat Commun* 2017; **8**: 14639.
- 26 Li P, Wei G, Cao Y, Deng Q, Han X, Huang X, Huo Y, He Y, Chen L, Luo J. Myosin IIa is critical for cAMP-mediated endothelial secretion of von Willebrand factor. *Blood* 2018; **131**: 686–98.
- 27 Michaux G, Abbitt KB, Collinson LM, Haberichter SL, Norman KE, Cutler DF. The physiological function of von Willebrand’s factor depends on its tubular storage in endothelial Weibel-Palade bodies. *Dev Cell* 2006; **10**: 223–32.
- 28 Romani de Wit T, Rondaij MG, Hordijk PL, Voorberg J, van Mourik JA. Real-time imaging of the dynamics and secretory behavior of Weibel-Palade bodies. *Arterioscler Thromb Vasc Biol* 2003; **23**: 755–61.

- 29 Riedl J, Crevenna AH, Kessenbrock K, Yu JH, Neukirchen D, Bista M, Bradke F, Jenne D, Holak TA, Werb Z, Sixt M, Wedlich-Soldner R. Lifeact: a versatile marker to visualize F-actin. *Nat Methods* 2008; **5**: 605–7.
- 30 Lui-Roberts WW, Collinson LM, Hewlett LJ, Michaux G, Cutler DF. An AP-1/clathrin coat plays a novel and essential role in forming the Weibel-Palade bodies of endothelial cells. *J Cell Biol* 2005; **170**: 627–36.
- 31 Blagoveshchenskaya AD, Hannah MJ, Allen S, Cutler DF. Selective and signal-dependent recruitment of membrane proteins to secretory granules formed by heterologously expressed von Willebrand factor. *Mol Biol Cell* 2002; **13**: 1582–93.
- 32 Knop M, Gerke V. Ca<sup>2+</sup>-regulated secretion of tissue-type plasminogen activator and von Willebrand factor in human endothelial cells. *Biochim Biophys Acta* 2002; **1600**: 162–7.
- 33 van der Walt S, Schonberger JL, Nunez-Iglesias J, Boulogne F, Warner JD, Yager N, Gouillart E, Yu T, scikit-image contributors. scikit-image: image processing in Python. *PeerJ* 2014; **2**: e453.
- 34 Tsai W. Moment-preserving thresholding: a new approach. In: O’Gorman L, Kasturi R, eds. *Document Image Analysis*. Los Alamitos, CA: IEEE Computer Society Press, 1995: 44–60.
- 35 Team RDC. *R: A Language and Environment for Statistical Computing*. R Foundation for Statistical Computing, 2011. www.R-project.org/ Accessed 16 February 2016
- 36 Forscher P, Smith SJ. Actions of cytochalasins on the organization of actin filaments and microtubules in a neuronal growth cone. *J Cell Biol* 1988; **107**: 1505–16.
- 37 Sanders YV, Groeneveld D, Meijer K, Fijnvandraat K, Cnossen MH, van der Bom JG, Coppens M, de Meris J, Laros-van Gorkom BA, Mauser-Bunschoten EP, Leebeek FW, Eikenboom J, Wi Nsg. von Willebrand factor propeptide and the phenotypic classification of von Willebrand disease. *Blood* 2015; **125**: 3006–13.
- 38 Straight AF, Cheung A, Limouze J, Chen I, Westwood NJ, Sellers JR, Mitchison TJ. Dissecting temporal and spatial control of cytokinesis with a myosin II inhibitor. *Science* 2003; **299**: 1743–7.
- 39 Michaux G, Pullen TJ, Haberichter SL, Cutler DF. P-selectin binds to the D<sup>1</sup>-D<sup>3</sup> domains of von Willebrand factor in Weibel-Palade bodies. *Blood* 2006; **107**: 3922–4.
- 40 Padilla A, Moake JL, Bernardo A, Ball C, Wang Y, Arya M, Nolasco L, Turner N, Berndt MC, Anvari B, Lopez JA, Dong JF. P-selectin anchors newly released ultralarge von Willebrand factor multimers to the endothelial cell surface. *Blood* 2004; **103**: 2150–6.
- 41 Kiskin NI, Hellen N, Babich V, Hewlett L, Knipe L, Hannah MJ, Carter T. Protein mobilities and P-selectin storage in Weibel-Palade bodies. *J Cell Sci* 2010; **123**: 2964–75.
- 42 McCormack JJ, Lopes da Silva M, Ferraro F, Patella F, Cutler DF. Weibel-Palade bodies at a glance. *J Cell Sci* 2017; **130**: 3611–7.
- 43 Valentijn KM, van Driel LF, Mourik MJ, Hendriks GJ, Arends TJ, Koster AJ, Valentijn JA. Multigranular exocytosis of Weibel-Palade bodies in vascular endothelial cells. *Blood* 2010; **116**: 1807–16.
- 44 Michaux G, Hewlett LJ, Messenger SL, Goodeve AC, Peake IR, Daly ME, Cutler DF. Analysis of intracellular storage and regulated secretion of 3 von Willebrand disease-causing variants of von Willebrand factor. *Blood* 2003; **102**: 2452–8.
- 45 Nightingale TD, Cutler DF, Cramer LP. Actin coats and rings promote regulated exocytosis. *Trends Cell Biol* 2012; **22**: 329–37.
- 46 Miklavc P, Wittekindt OH, Felder E, Dietl P. Ca<sup>2+</sup>-dependent actin coating of lamellar bodies after exocytotic fusion: a prerequisite for content release or kiss-and-run. *Ann N Y Acad Sci* 2009; **1152**: 43–52.
- 47 Yu HY, Bement WM. Control of local actin assembly by membrane fusion-dependent compartment mixing. *Nat Cell Biol* 2007; **9**: 149–59.
- 48 Lorenzi O, Frieden M, Villemin P, Fournier M, Foti M, Vischer UM. Protein kinase C-delta mediates von Willebrand factor secretion from endothelial cells in response to vascular endothelial growth factor (VEGF) but not histamine. *J Thromb Haemost* 2008; **6**: 1962–9.
- 49 Jabbour G, Lemoine-Morel S, Casazza GA, Hala Y, Moussa E, Zouhal H. Catecholamine response to exercise in obese, overweight, and lean adolescent boys. *Med Sci Sports Exerc* 2011; **43**: 408–15.
- 50 Cho W. Membrane targeting by C1 and C2 domains. *J Biol Chem* 2001; **276**: 32407–10.
- 51 Khaliulini I, Bond M, James AF, Dyar Z, Amini R, Johnson JL, Suleiman MS. Functional and cardioprotective effects of simultaneous and individual activation of protein kinase A and Epac. *Br J Pharmacol* 2017; **174**: 438–53.
- 52 Yang W, Mei FC, Cheng X. EPAC1 regulates endothelial annexin A2 cell surface translocation and plasminogen activation. *FASEB J* 2018; **32**: 2212–22.
- 53 Aslam M, Tanislav C, Troidl C, Schulz R, Hamm C, Gunduz D. cAMP controls the restoration of endothelial barrier function after thrombin-induced hyperpermeability via Rac1 activation. *Physiol Rep* 2014; **2**(10): e12175.
- 54 Conte IL, Cookson E, Hellen N, Bierings R, Mashanov G, Carter T. Is there more than one way to unpack a Weibel-Palade body? *Blood* 2015; **126**: 2165–7.
- 55 Kaufmann JE, Oksche A, Wollheim CB, Gunther G, Rosenthal W, Vischer UM. Vasopressin-induced von Willebrand factor secretion from endothelial cells involves V2 receptors and cAMP. *J Clin Invest* 2000; **106**: 107–16.